

Utah State University

DigitalCommons@USU

---

All Graduate Theses and Dissertations, Fall  
2023 to Present

Graduate Studies

---

8-2024

## Computational Fluid Dynamics Modeling of Air Demand for Fixed Cone Valve in Energy Dissipating Structure

Matthew S. Harames  
*Utah State University*

Follow this and additional works at: <https://digitalcommons.usu.edu/etd2023>



Part of the [Civil and Environmental Engineering Commons](#)

---

### Recommended Citation

Harames, Matthew S., "Computational Fluid Dynamics Modeling of Air Demand for Fixed Cone Valve in Energy Dissipating Structure" (2024). *All Graduate Theses and Dissertations, Fall 2023 to Present*. 220. <https://digitalcommons.usu.edu/etd2023/220>

This Thesis is brought to you for free and open access by the Graduate Studies at DigitalCommons@USU. It has been accepted for inclusion in All Graduate Theses and Dissertations, Fall 2023 to Present by an authorized administrator of DigitalCommons@USU. For more information, please contact [digitalcommons@usu.edu](mailto:digitalcommons@usu.edu).



COMPUTATIONAL FLUID DYNAMICS MODELING OF AIR DEMAND FOR  
FIXED CONE VALVE IN ENERGY DISSIPATING STRUCTURE

by

Matthew S. Harames

A thesis submitted in partial fulfillment  
of the requirements for the degree

of

MASTER OF SCIENCE

in

Civil and Environmental Engineering

Approved:

---

Michael C. Johnson, Ph.D., P.E.  
Major Professor

---

Zachary B. Sharp, Ph.D., P.E.  
Committee Member

---

J. Burdette Barker, Ph.D., P.E.  
Committee Member

---

D. Richard Cutler, Ph.D.  
Vice Provost of Graduate  
Studies

UTAH STATE UNIVERSITY  
Logan, Utah

2024

Copyright © Matthew S. Hames 2024

All Rights Reserved

## ABSTRACT

Computational Fluid Dynamics Modeling of Air Demand For Fixed Cone Valve In  
Energy Dissipating Structure

by

Matthew S. Harames, Master of Science

Utah State University, 2024

Major Professor: Dr. Michael C. Johnson  
Department: Civil and Environmental Engineering

Fixed cone valves are commonly installed as low-level outlet devices to discharge flow from reservoirs. Fixed cone valves offer good control and dissipate energy through dispersion unless the discharging flow is contained in a hood or energy dissipating structure. As water is discharged out of a fixed cone valve into a hood or energy dissipating structure, air flow is required for proper operation of the valve. There is currently a lack of published information needed to estimate the demand for air flow for such installations. Furthermore, using model studies or computational fluid dynamics (CFD) simulations may be used but the results of such have not been verified nor is information publicly available in the literature. The purpose of this research was to perform a model-to-prototype comparison for fixed cone valve and associated energy dissipating structure air demand and quantify, using CFD simulation, air demand for a fixed cone valve installed in such a structure.

Data regarding air flow demand was collected from a prototype fixed cone valve and energy dissipating structure. A physical scale model was built at Utah Water Research Laboratory and similar data were collected from the physical model. In addition, CFD modeling was also performed on a three-dimensional model of the energy dissipating structure.

In this physical model study, the demand for air flow was not properly captured using Froude similitude. A comparison between the prototype data and the results generated from the CFD simulation shows promise for capturing the air demand of fixed cone valves in energy dissipating structures and perhaps for other structure types where flowing water induces air demand. Further increases in computational power may allow CFD to be a viable alternative in the future. This research is significant because it provides a direct comparison between a model's and a prototype's air demand and provides evidence that CFD modeling has promise as a viable alternative to model studies.

(48 pages)

## PUBLIC ABSTRACT

Computational Fluid Dynamics Modeling of Air Demand For Fixed Cone Valve In  
Energy Dissipating Structure

Matthew S. Harames

Fixed cone valves are commonly installed as low-level outlet devices to discharge water from reservoirs. When discharging water, the fixed cone valves require an air vent to properly operate and maintain the valve. There is a current lack of published information regarding the accuracy of model studies to properly estimate the air demand on the full-size prototype. This research aims to help close that gap by providing data comparison between a model and prototype. Furthermore, computational fluid dynamics (CFD) simulations may be used to estimate the air demand, but the results of such have not been verified nor is information publicly available in the literature. Along with the model-to-prototype comparison, this research aims to investigate the accuracy of using CFD to estimate the air demand.

The result of this study provides a rare comparison of model and prototype data. Providing evidence that predicting air demand in the prototype from a model study is not reliable. A comparison between a CFD simulation and the data collected from the field was also performed. Providing evidence that CFD may be a viable alternative with future increases of computational power.

## ACKNOWLEDGMENTS

I would like to thank Dr. Michael Johnson for accepting me to be his graduate student and being a mentor in my journey into civil engineering. I would also like to thank him for supporting me and providing guidance throughout this research.

Thanks to Zac Sharp who helped provide guidance with the running and operating of the CFD model.

Additional thanks to Burdette Barker for reviewing the manuscript and providing clarifying contributions and advice on formatting.

I would also like to thank Stephen Sanders and Tyler Mindrum for helping me collect in the field. I'd also like to thank them for the countless hours they used to help build and test the model.

Finally, I'd like to thank my wife Rebecca in supporting me in this journey. It wouldn't have been possible without her encouragement and personal sacrifices.

Matthew S. Harames

## CONTENTS

	Page
ABSTRACT.....	iii
PUBLIC ABSTRACT.....	v
ACKNOWLEDGMENTS .....	vi
LIST OF TABLES .....	viii
LIST OF FIGURES .....	ix
LIST OF EQUATIONS.....	x
NOTATION.....	xi
CHAPTER I INTRODUCTION.....	1
Statement Of The Problem.....	1
Purpose Of The Study .....	3
CHAPTER II LITERATURE REVIEW .....	4
CHAPTER III METHODOLOGY .....	7
Prototype Data Collection.....	7
Model Data Collection.....	11
Data Handling and Analysis.....	13
Computational Fluid Dynamics .....	16
CHAPTER IV RESULTS AND DISCUSSION .....	24
Prototype Data .....	24
Model Data.....	25
CFD Data .....	28
Prototype and Model Analysis .....	30
Prototype and CFD Analysis.....	32
CHAPTER V CONCLUSIONS.....	35
REFERENCES .....	37



## LIST OF TABLES

<b>Table 1</b> Air Inlet Velocity Data Collected from Prototype. ....	24
<b>Table 2</b> Air Inlet Velocity Data Collected from Scale Model. ....	26
<b>Table 3</b> Data Obtained from CFD Model (feet per second). ....	29
<b>Table 4</b> Calculated Air Flow Rates (Cubic Feet per Second). ....	30
<b>Table 5</b> Physical Model Data and Scaled via Froude Similitude. Includes Calculated Scale Effect. ....	31
<b>Table 6</b> CFD and Prototype Air Velocity Comparisons. ....	33

## LIST OF FIGURES

<b>Figure 1</b> Geometry of energy dissipation structure.....	8
<b>Figure 2</b> Air grate at energy dissipating structure. ....	10
<b>Figure 3</b> Kanomax A031 hot-wire anemometer. ....	10
<b>Figure 4</b> Picture of model at Utah Water Research Laboratory. ....	12
<b>Figure 5</b> Air grate on model. ....	13
<b>Figure 6</b> Example of spline-interpolated velocity for a prototype measurement (Column 3 in Table 1). ....	15
<b>Figure 7</b> 3D CFD model of the energy dissipating structure fluid volume.....	19
<b>Figure 8</b> Slice of mesh generated for CFD model. ....	22
<b>Figure 9</b> Velocity seen at air-water boundary in CFD model.....	23
<b>Figure 10</b> Spline-interpolated velocity for a prototype measurement (Column 4 in Table 1). ....	25
<b>Figure 11</b> Spline-interpolated velocity for a model measurement (Column 3 in Table 2). ....	27
<b>Figure 12</b> Spline-interpolated velocity for a model measurement (Column 4 in Table 2). ....	27
<b>Figure 13</b> Spline-interpolated velocity for CFD measurement (Table 3). ....	29
<b>Figure 14</b> Air velocity measurement using built in CFD tool.....	30

## LIST OF EQUATIONS

<b>Equation 1</b> Air Velocity Conversion .....	14
<b>Equation 2</b> Continuity Equation. ....	17
<b>Equation 3</b> Momentum Equation.....	17
<b>Equation 4</b> Courant Number.....	21

## NOTATION

$U_m$ : Actual air velocity

$p_m$ : Atmospheric air pressure at time of reading

$U_c$ : Air velocity reading

$C$ : Courant number

$U$ : Velocity of fluid particle

$\Delta t$ : Time step

$\Delta x$ : Characteristic length of mesh cell

$t$ : Time

$p$ : Pressure

$\mu$  : Kinematic Viscosity

$\vec{V}$ : Continuum Velocity

$\rho$ : Density

## CHAPTER I

### INTRODUCTION

#### **Statement Of The Problem**

Fixed cone valves (also called Howell-Bunger valves) are commonly used to control the releases through the low-level outlet works of dams and are also used to bypass flow when needed for hydropower installations. As the water exits the conduit via the fixed cone valve, the conical jet of water has a high velocity that entrains and carries air with it downstream. This creates a low-pressure zone at the exit of the fixed cone valve, allowing air to flow from an area of higher pressure to this newly created low-pressure zone. This requires a supply of air to mitigate the low-pressure zones in the flow, which otherwise could lead to cavitation and may result in cavitation damage.

Consequently, when designing outlet works that will include fixed cone valves, an air vent is imperative to include (Falvey, 1980). This need is not needed for fixed cone valves discharging directly to atmosphere where adequate air exists, however for fixed cone valves installed with hoods or in conjunction with energy dissipating structures, an adequate supply of air mitigates hydraulic issues associated with unsatisfied air demand.

There are a handful of different considerations when designing the shape and size of an air vent, however the focus is generally the air velocity. Air velocities that are too high can cause objectional noise. It is recommended to keep air velocities in duct work below 300 feet per second (Colgate, 1963). Since air velocity is a function of the air demand and area of the air supply conduit, accurate estimates of the air demand created by the fixed cone valve need to be made. These estimates are usually calculated through model studies, however the accurate prediction of air demand via these model studies

have not been proven and model-to-prototype comparisons are lacking (Colgate, 1963). A primary cause of physical model air demand uncertainty is the nature of the governing forces involved. Froude modeling identifies the predominant forces acting on the water as inertia and gravity while the air movement for the prototype and scale model is driven by pressure forces which would indicate that pressure and inertia forces govern its movement indicating Euler scaling would be appropriate. However, Euler scaling does not have a length ratio and generally takes the form of a dimensionless parameter such as a discharge coefficient.

Because air vents may be used for access to perform maintenance on the dam by staff or be in the vicinity of where people may work, having confidence in the air demand is paramount to designing an air vent that keeps velocities at a safe and permissible level. An example showing the need to keep the air velocities within a safe level is an accident that occurred at the Oroville dam in 2009. Due to a failure of a pressure wall separating the staff from the tunnel that housed operating fixed cone valves, five employees suffered injuries due to the force of the air flow generated by fixed cone valves (Scott, 2010).

One potential approach to quantifying the air demand of a fixed cone valve in an energy dissipating structure would be to use a Computational Fluid Dynamics (CFD) software package to computationally model the outlet works. CFD is an area of fluid mechanics that uses numerical methods to approximate and model fluid flows. It is a useful tool to study and model systems and phenomena that would be otherwise impossible or impractical to test.

## **Purpose Of The Study**

The aim of this study is to provide a physical model-to-prototype comparison of the air demand and to investigate how well the physical model does at predicting the prototype air demand. Along with providing a unique opportunity to have model-to-prototype comparison data, a CFD study using the commercial software Star-CCM+ (Siemens Digital Industries Software, Plano, TX), was performed. The primary research tasks were as follows:

- 1) Complete a thorough literature review of research regarding air demand in fixed cone valves.
- 2) Collect physical data from 78-inch fixed cone valves installed in an energy dissipating structure.
- 3) Collect physical data from a 10 scale Froude model of the energy dissipating structure.
- 4) Collect CFD data by running a simulation of the energy dissipating structure at the operating conditions from which the data were collected.
- 5) Analyze the data collected from the prototype and physical model to understand a potential scale effect.
- 6) Analyze the data collected from the CFD model to determine if using CFD software is a potential alternative to assessing air demand in fixed cone valves.

## CHAPTER II

### LITERATURE REVIEW

A literature review was performed to find relevant papers discussing air demand from fixed cone valve installations. No literature regarding the comparison of a model study to a prototype was able to be found. It is possible that information does exist, however it is not publicly available.

Elder and Dougherty (1953) conducted a study on different hydraulic characteristics of fixed cone valves installed by the Tennessee Valley Authority. For the Fontana and Watauga dam installations, one of the characteristics studied was of the air demand condition. It is noted in the paper that air demand is a function of the structure surrounding the valve and any specific values obtained apply only to structures that are built identical to the structure studied. The authors note that based on the fundamental equations of continuity, it is expected that air demand will increase with larger sleeve openings. However, the data they observed from the Fontana and Watauga installations indicated a maximum air demand when valves were around eight to ten percent open. They explain this with a visual observation that a secondary back flow and splash formed a curtain over the air intake, limiting the flow of air. It was observed that when the valves were completely smothered by the splash, air demand was minimized.

Colgate (1963) under the direction of the United States Bureau of Reclamation (USBR) conducted a model study at the USBR Hydraulic Laboratory in Denver, Colorado for Tunnel No. 2 at Oroville Dam in California. During this model study, an estimation of air demand for the twin fixed cone valves was performed so an adequate air vent size could be designed. This was done by correlating the ratio of the air demand and



the water discharging from the valve to the air pressure at the bulkhead. Data were collected across a range of flow rates and valve openings to create this relationship. The laws of Froude similitude were used to scale the data collected from the model to the prototype. He specifically mentions that the accuracy of predicting air demand using scale models has not been proven.

Falvey (1980), working at the USBR later built upon the work done by Colgate. Using the relationship developed by Colgate, Falvey transformed the values into dimensionless parameters that represent the relative air pressure at the valve and relative air flow rate. Using an equation to find the dimensionless air flow rate for any given air vent, that equation can be plotted onto a transformed figure similar to the one Colgate developed. This allows for the determination of the air flow rate of any vent attached to the structure the figure was developed for. This notion implies that during the design phase, an engineer could estimate the air demand for a multitude of air vents; But this contradicts the findings from Elder and Dougherty (1953) that the air demand is a function of the structure surrounding the valve. Modifying the air vent is directly modifying the structure and thus should modify the air demand according to Elder and Dougherty.

Calderon et al. (2018), using CFD simulation to estimate the air demand in an outlet works using radial gates at Ituango Dam in Antioquia, Colombia. These gates obviously differ from the fixed cone valves being studied in the present research. However, no literature involving using CFD to estimate air demand in fixed cone valves was found. Calderon et al. presented a few common equations developed to estimate the air demand using the Froude Number at the vena contracta of the gate. They then

simulated water releases at different gate openings and pressures, calculating the air demand required by operation of the radial gates. The authors found that the CFD simulation performed similarly to already established empirical equations for radial gates. Upon completion of the project, data collected from the field was to be collected and compared to the CFD results. However, the Ituango Project construction was not finished at the time of this writing (ca. 2024).

The previous paragraphs summarize all the relevant literature found regarding estimating air demand for fixed cone valves in hydraulic structures and using CFD to estimate air demand for hydraulic structures. There is limited publicly available data and research on air demand for fixed cone valves and the intent of this study is to make available additional information and options for this important topic.

## CHAPTER III

### METHODOLOGY

#### **Prototype Data Collection**

The prototype that was selected for data collection is outfitted with two 78-inch fixed cone valves housed inside of an energy dissipating structure. There are mirrored energy dissipating structures with having the fixed cone valve centered laterally in the chamber and positioned such that the jet is intercepted by the side walls, ceiling and floor. The chamber has a deflector on each wall and ceiling and an end sill on the floor at the exit of the structure. An image showing a 3D model of the inside of one chamber is seen in Figure 1. The fixed cone valve is seen intruding into the energy dissipation structure on the left-hand side with the air grate above it. On the right-hand side the outlet to the structure can be seen. In the prototype, the outlet was emptying into a downstream river.

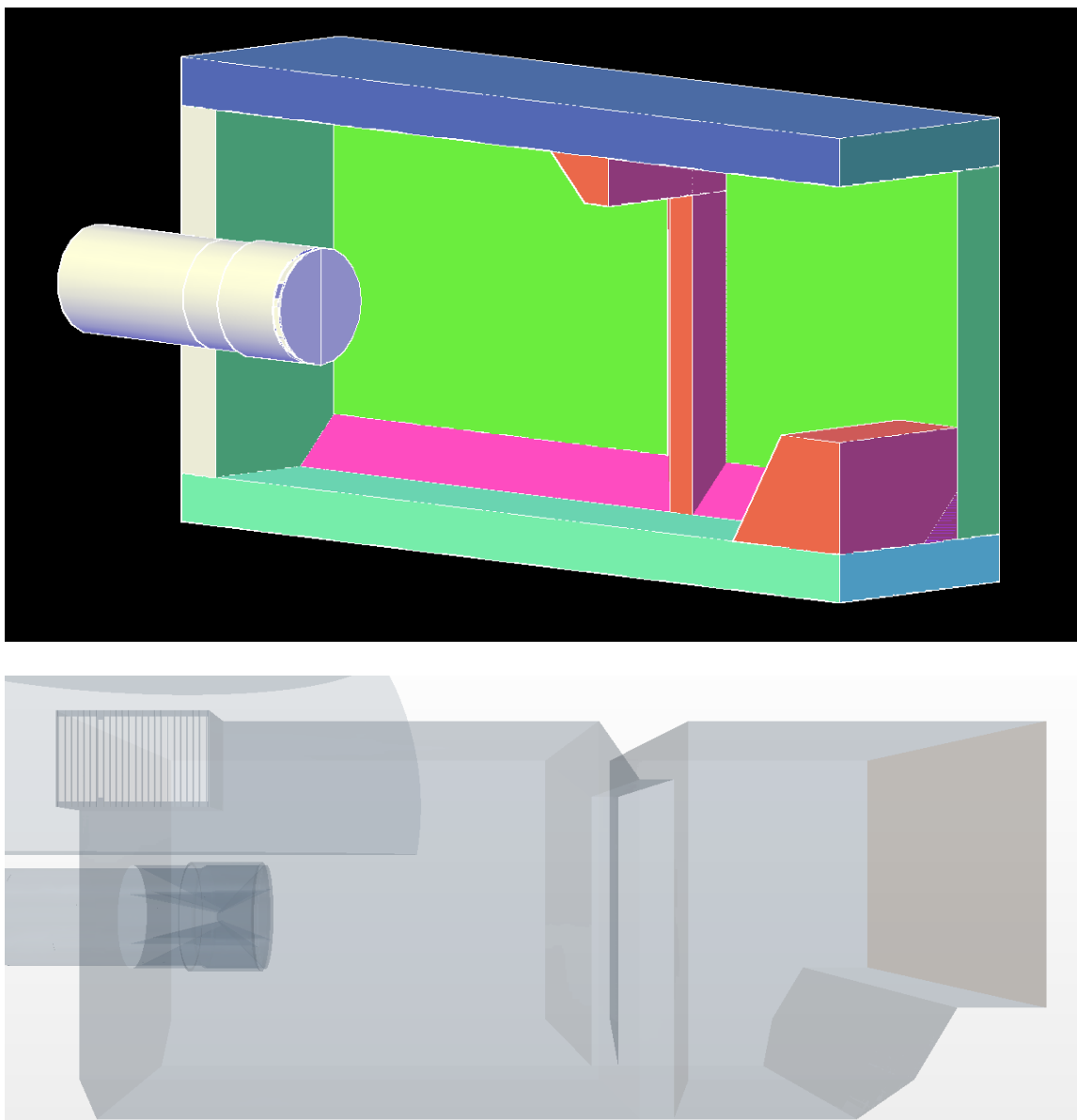


**Figure 1** *Geometry of energy dissipation structure.*

The data was collected on June 21<sup>st</sup>, 2023, and consisted of twelve, point air-velocity measurements at the grated opening that allows air flow required by each energy dissipating chamber and its associated valve. The grate opening measures 8 feet by 4.375 feet with each bar being 0.75 inches wide with 3.25 inches between bars. Figure 2 shows a picture of the grate with the blue masking tape denoting where the velocity measurements were made. Each measurement was made between the bars on the left side

of the masking tape. The instrument used was a Kanomax (Andover, New Jersey) Model A031 hot wire anemometer as seen in Figure 3. Measurements were taken for two identical chambers and valves as the structure had a mirror layout with each valve isolated in its own chamber. Discharge for each valve was obtained from the monitoring equipment located in the nearby control room at 570 cfs passing through each fixed cone valve. From the discharge values and information obtained from the dam operator about the intake system, the pressure at the fixed cone valves was calculated to be 114 psi. Additional measurements at other flows could not be obtained due to operational restrictions at the reservoir.

Due to the nature of hot-wire anemometers, any water splashing onto the hot-wire may result in erroneously high measurements. However, due to the high air velocities seen on site, splashing near the grate was minimal and didn't affect the readings. On the day of the readings, no strong winds were observed that could've affected the data. Another potential uncertainty in the data collected, is if the grid chosen is representative of the air flow across the entire grate. Finally, the two chambers may not be identical due to unknown differences resulting from construction in either the surrounding energy dissipation structure or the fixed cone valve itself.



**Figure 2** *Air grate at energy dissipating structure.*

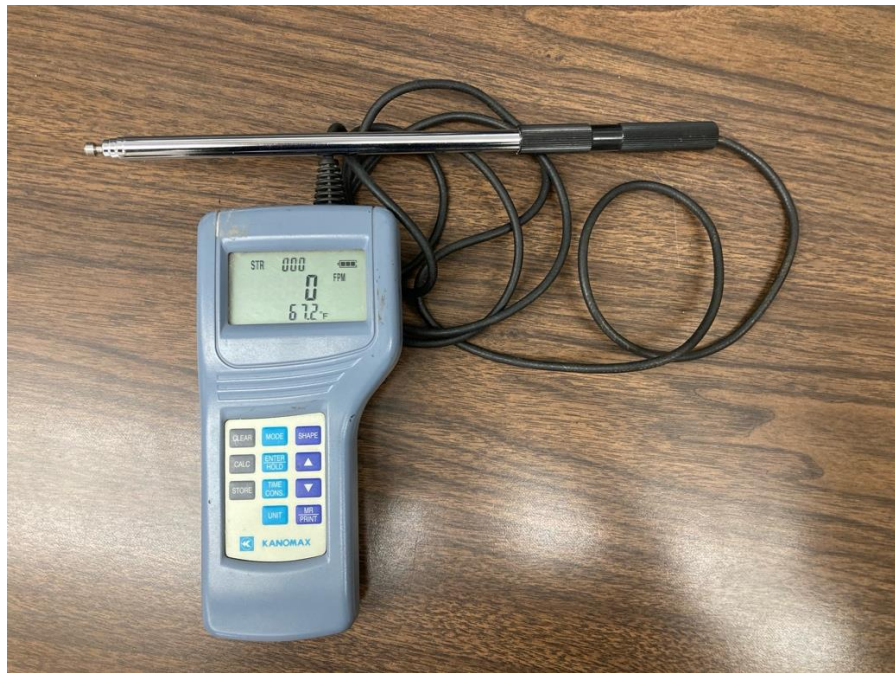


**Figure 3** *Kanomax A031 hot-wire anemometer.*

## Model Data Collection

The model built was roughly a 10:1 (78/7.83) scale Froude model. This scale was chosen because Utah Water Research Laboratory had an existing 7.83-inch fixed cone valve to build around. A Froude model was chosen for a variety of reasons. Physical modeling requires choosing a model that best represents the forces at play on the different fluids. When considering the water, gravity and inertia are the main forces at play, making a Froude model an ideal candidate. However, the air is dominated by pressure and inertial forces. The differing forces at play on the two fluids can not be satisfied at the same time. Other models, such as a Reynolds model were not chosen due to physical limitations of equipment available for modeling. The necessary flow volume for the water in a Reynolds model was not physically achievable. Using a Froude model also follows the work done by Colgate (1963) and the subsequent work by Falvey (1980).

The model was built at Utah Water Research Laboratory and consisted of the fixed cone valve and the associated energy dissipating structure. As mentioned previously, the two fixed cone valves are isolated in mirrored chambers, so a decision was made to only model half of the outlet works. This was done both to simplify the model itself and due to the limitation of only having one fixed cone valve to use in testing. Figure 4 shows an image of the model. The plywood below the grate is to simulate the ground surface seen in the prototype, as a large portion of the energy dissipating structure was below the ground's surface.



**Figure 4** *Picture of model at Utah Water Research Laboratory.*

Data was collected on August 11, 2023, using a similar method as the prototype data collection. The same Kanomax A031 hot wire anemometer was used to measure the air velocity in twelve different point locations. Figure 5 shows the point locations marked in sharpie, highlighted in yellow for easier viewing. The locations are in the same relative position when compared to the prototype. Using Froude similitude, the discharge was calculated to be 817 gallons per minute and the pressure in the fixed cone valve was set to 11.4 psi. The data points were collected twice to have the same number of observations as obtained from the prototype.

It should be noted that the model experienced a lot of splashing of water at the grate. With the way hot-wire anemometers measure air flow, any water splashing onto the



wire could've altered the measurement. Water getting directly onto the hot-wire was minimized as much as was feasible. The model experienced low air velocities and any air drafts in the laboratory could've also modified the data. However, the researchers didn't note any noticeable air drafts at the time of collection.

Due to the low air velocities and splashing seen at the grate, an additional measurement using a tube placed around the grate was obtained to verify the results of the total air demanded.



**Figure 5** *Air grate on model.*

### **Data Handling and Analysis**

The data was collected and transposed into a CSV file named DataCollected.CSV. The file can be accessed from a public GitHub repository (Harames, 2024). This CSV file

consisted of the following columns, model, flow rate, psi, and air flow for each of the 12 measurements. The model column has either a 1 or a 0, with 1 denoting the measurement were obtained from the model and 0 from the prototype. Flow rate refers to the flow rate of the water exiting the fixed cone valve in cubic feet per second. psi is the pressure in the fixed cone valve in pounds per square inch. Air flow is the measurements from the hot wire anemometer measured in feet per minute. The different points are numbered from 1 to 12, starting at the top left of the grate and incrementing to the right. Starting from the left, the top row of points are numbered 1, 2, 3, 4; middle row of points are 5, 6, 7, 8; and the bottom row of points are numbered 9, 10, 11, and 12. This numbering is consistent between both the prototype and model data.

The CSV file was imported into R Studio to perform preliminary modifications and adjustments to the structure before exporting a modified data set. The modifications include adjusting the air flow values (Equation 1) to account for differences in atmospheric pressure according to the Kanomax A031 user manual (Kanomax). The data was also converted from feet per minute to feet per second. The modified data was exported as ScaledData.CSV and can be accessed from the Github repository.

The velocity probe reports the velocity of air at the standard atmosphere. Because the air at the site and the laboratory are different than the standard atmosphere, corrections to accommodate for the air density must be made. The correction is given in Equation 1.

**Equation 1** *Air Velocity Conversion*

$$U_m = \frac{1013}{P_m} \times U_c$$

Where  $U_m$  is the actual air velocity,  $P_m$  is the atmospheric pressure at the time of sampling, and  $U_c$  is the air velocity reading.

To estimate a volumetric flow rate for the air demand, a form of integrating the values recorded over the area of the air grate is needed. This was done in Python 3.9.7 in a Jupyter Notebook. The Numpy library was used to import the scaled data and a program was written to store the pertinent data in a list. A function was written that uses the regular grid interpolator from the Scipy library to create a 2D piecewise Hermite cubic interpolating spline from the observed data. An example visualization using the Matplotlib library of the resulting spline can be seen in Figure 6. An assumption that the air flow rate at the boundary of the air grate is zero was made. This assumption will have the effect that the air flow rate between the boundary of the grate and the first observed data point will be underestimated.

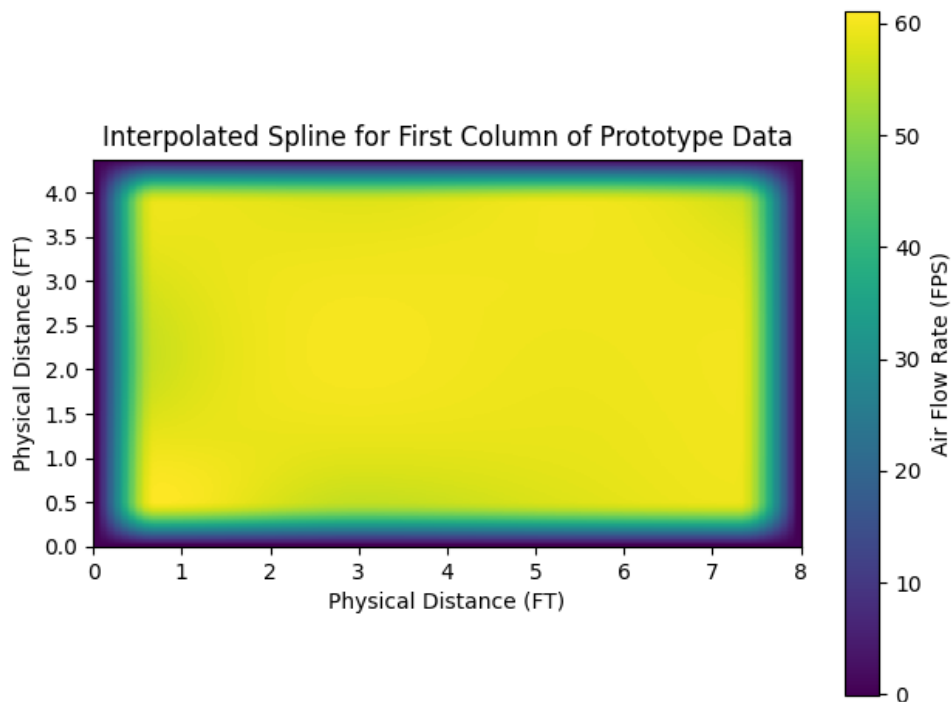


**Figure 6** Example of spline-interpolated velocity for a prototype measurement (Column 3 in Table 1).

With the interpolated cubic spline made, an estimated air flow rate for any point on the surface of the air grate can be found. To estimate the volumetric air flow rate, the function splits the surface up into 23 different sections along the x-axis. These spots correspond to the gaps between the grating. It also splits the surface up into 20 different sections along the y-axis. 20 was chosen to get good spatial resolution as there are no physical delimiters as seen when considering the x-axis. These two combined breaks the surface into 460 squares each one corresponding to a 3.25-inch by 2.625-inch square of space between the bars on the air grate seen on the prototype. The function also accepts a scale size parameter to adjust these lengths appropriately for the model data. Using these squares and the interpolated cubic spline, the function finds the interpolated air velocity in the center of each square, multiplies the area of the square by the air flow rate, and adds the resulting volumetric flow rate for each square together to estimate the volumetric flow rate for the entire air grate. The squares are spaced to avoid the bars, thus that area adds nothing to the total air flow. The Jupyter notebook and mentioned code can be accessed from the same GitHub repository as the CSV files (Harames, 2024).

For the uncertainty of the data, the air velocity data collected with the Kanomax A031 is with plus or minus 3% of the reading (Kanomax). The discharge and psi for the prototype are within plus or minus 1%. The flow meter at Utah Water Release Laboratory is accurate within plus or minus 0.25% and the pressure transmitter is within plus or minus 0.1%.

### **Computational Fluid Dynamics**

CFD modeling is based on solving the Navier-Stokes equations to track the movement of fluid particles throughout a domain. The Navier-Stokes equations consist of

an equation to track the continuity and momentum of the fluid particles. The general forms of the equations are given as:

**Equation 2** *Continuity Equation.*

$$\nabla \cdot \vec{V} = 0$$

**Equation 3** *Momentum Equation.*

$$\rho \frac{D \vec{V}}{Dt} = -\nabla p + \rho \vec{g} + \mu \nabla^2 \vec{V}$$

Where  $\rho$  is the density of the fluid,  $\vec{V}$  is the continuum velocity,  $t$  is time,  $p$  is pressure,  $g$  is gravity, and  $\mu$  is the kinematic viscosity.

Due to the nature of the Navier-Stokes equations being partial differential equations, a closed form analytical solution can't always be found. Using numerical methods and computers, the Navier-Stokes equations can be solved for complex geometries and scenarios. A common approach to help simplify the Navier-Stokes equations is to break the turbulence into a time independent value and a time dependent value. This is referred to as a Reynolds-Averaged Navier-Stokes (RANS) approach. Other approaches to resolve the turbulence term is a scale-resolving method such as Large Eddy Simulation (LES) or Detached Eddy Simulation (DES). However, both approaches require high computational cost that isn't feasible for this model (Siemens Digital Industries Software, 2018).

Due to the nature of this problem looking at air demand within a hydraulic dissipating chamber for fixed cone valves, additional equations are needed to track the two different fluids. There are a few approaches to tracking multiple fluids, also called multiphase flow, such as an Eulerian approach, Lagrangian approach, and a Eulerian-Lagrangian approach. The Eulerian approach tracks the different computational values in

each individual cell throughout the computational domain. In contrast, the Lagrangian approach tracks individual fluid particles as they move through the computational domain. The Eulerian approach was chosen due to it being less computationally expensive to perform. To track the different phases, a volume of fluid approach is chosen. A volume of fluid tracks the percentage of water and air inside each cell, instead of tracking the individual fluid particles. This has the benefit of speeding up computational time.

The CFD modeling was performed at Utah Water Research Laboratory using Star-CCM+ 13.06.012-R8. A 3D model of the energy dissipating structure was created in AutoCAD and exported to an IGES file. The gate on the fixed cone valve was exported separately to allow positioning within Star-CCM+. The IGES files were imported into Star-CCM+ and boundary conditions were set, a picture of the 3D model can be seen in Figure 7.

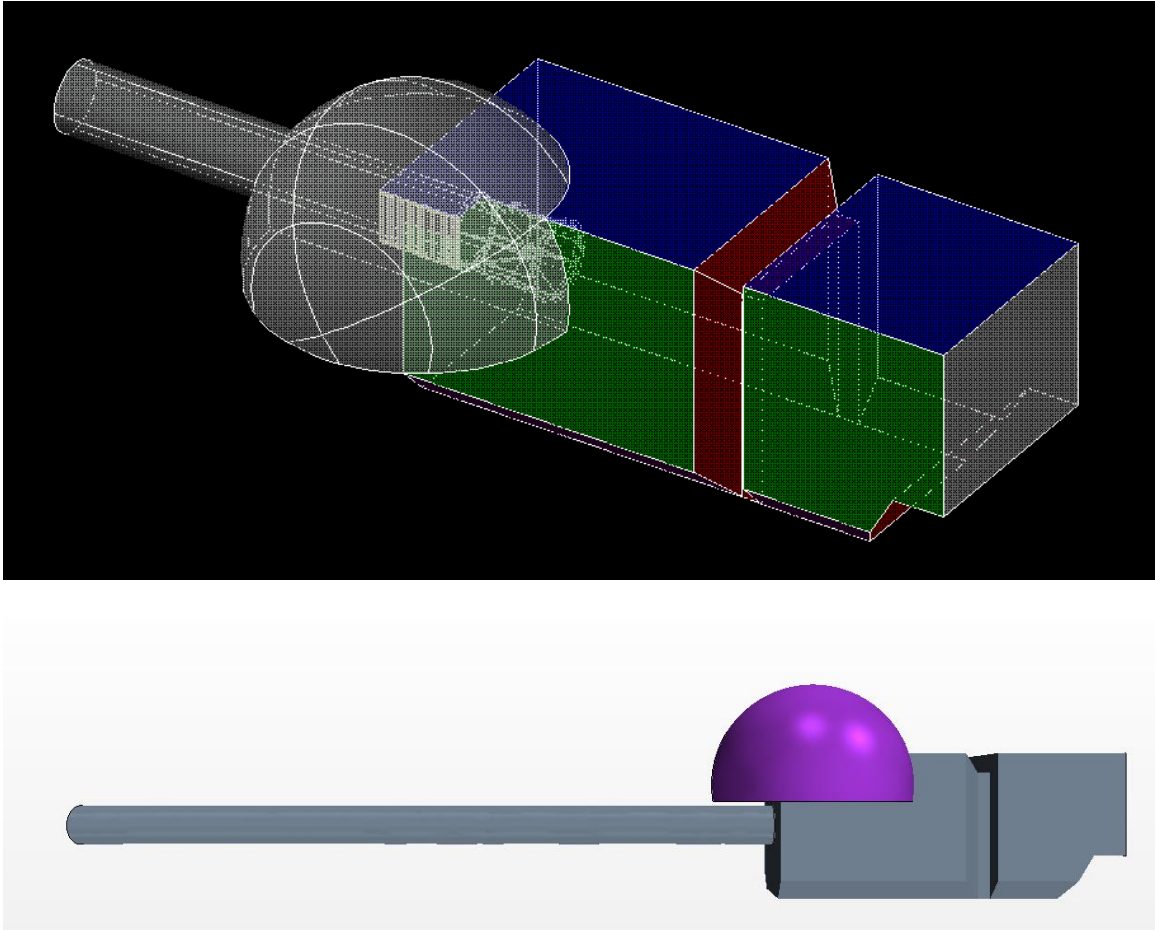


**Figure 7** 3D CFD model of the energy dissipating structure fluid volume.

The boundary conditions were set as follows: on the pipe intake a mass inflow was set to 35497.15 pounds per second to achieve the 570 cubic feet per second of flow seen in the prototype. The quarter sphere, purple in Figure 7, was set to a stagnation inlet to allow for air flow into the structure. The outlet was set to a pressure outlet. Every other boundary was set as a wall having the no-slip boundary condition.

CFD software can use a multitude of different numerical models to calculate turbulence and multiphase flow. For this simulation a choice of the following models were selected:

- Three-dimensional,

- Implicit unsteady,
- Eulerian multiphase,
- Volume of fluid (VOF),
- Turbulent,
- K-Epsilon turbulence
- Reynolds-Averaged Navier-Stoke (RANS),
- Gravity
- Two-layer all  $y^+$  wall treatment,
- Exact wall distance,
- Realizable K-Epsilon two-layer,
- Gradients,
- Segregated flow, and
- Multiphase interaction.

The most important role in every CFD simulation is the mesh that is produced. A mesh splits up the computational domain into cells wherein all the different equation calculations for each is completed using information from the surrounding cells. It is imperative that the mesh is of proper density, otherwise convergence of a solution may not be possible. The meshing models chosen included: trimmer, surface remesher, and prism layer mesher. A limitation of the trimmer mesh is the cell expansion when changing from one cell size to another. This can be mitigated using a polyhedral mesh, but the trimmer mesh was chosen to capture the sharp corner seen in the fixed cone valve. A future study looking at using a polyhedral mesh instead may yield different results. The base cell size chosen was 1 ft, with a relative minimum size of 0.05 ft, and a relative



target size of 0.1 ft. However, due to the relatively small size of the gate opening in the fixed cone valve, volumetric controls were used to shrink the cells around the gate opening, down to a size of 0.015 ft. Figure 8 shows a slice of the mesh generated around the gate opening, notice the higher cell density the closer to the opening. Due to the high cell density, the time step used in the model needs to be small enough to prevent convergence issues. It is recommended that the Courant number is kept equal or below 1. The Courant number is defined as below and if it is greater than 1, then a fluid particle will jump across multiple cells in a single time step.

**Equation 4** *Courant Number*

$$C = \frac{U \Delta t}{\Delta x}$$

Where  $U$  is the velocity of the fluid particle,  $\Delta t$  is the time step, and  $\Delta x$  is the characteristic length of the cells. Since the smallest cell size is 0.015 ft, a time step of  $5e^{-5}$  seconds was chosen as velocities around 300 feet per second were seen in a few cells. For each time step, an inner iteration of 15 was chosen as that provided good convergence for each step observed. The model was initialized with air throughout the domain and the model operator waited until the pipe filled with water. The pressure at the fixed cone valve was checked and the position of the gate was moved if the pressure didn't reach the target 114 psi. The model was remeshed and the solution interpolated onto the new mesh. This process was repeated, moving the position of the gate, until the 114 psi target was reached. The model was allowed to run until it appeared that the mass volume flow across the stagnation inlet had converged. The generated mesh had over 24 million computation cells and the entire process took five months of real time to obtain a solution. In hindsight, obtaining access to a high-performance computing (HPC) platform

to speed up the simulation should have been done. The computer used had twenty CPU cores and 64 Gigabytes of RAM, which clearly was not adequate to obtain a timely solution. Figure 9 shows the water-air surface of the CFD model as the jet of water is exiting the fixed cone valve.

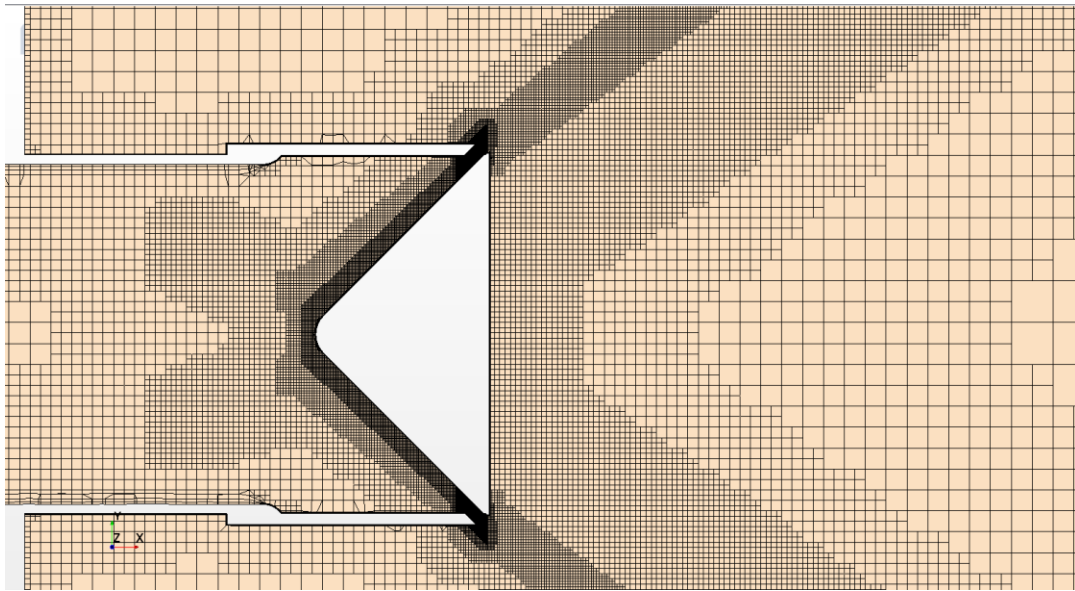


**Figure 8** *Slice of mesh generated for CFD model.*

For obtaining the air demand from the CFD model, two methods were used. One is using the mass flow function built into Star-CCM+ on the quarter sphere stagnation inlet and calculating the resulting air flow using the density set in the model. The second is creating twelve point monitors and calculating the air velocity for each point. From there the points can be put into the Jupyter Notebook code and the volumetric air volume can be calculated the same way as the other data. Using these two methods allows one to check to see if the interpolating spline gives realistic estimates for the air flow.

Uncertainty in CFD simulations is usually calculated using a grid convergence test. However, as mentioned previously, due to computational and time restrictions, a grid

convergence test was unable to be performed.

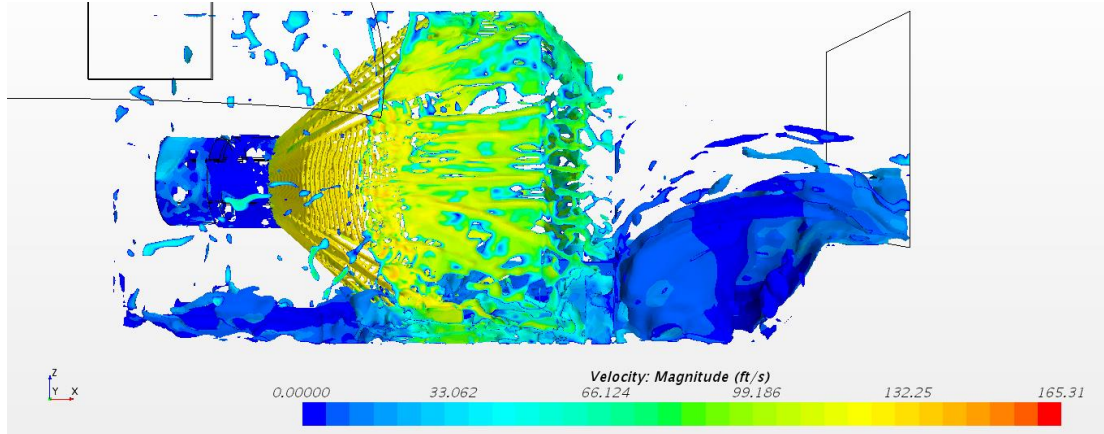


**Figure 9** *Velocity seen at air-water boundary in CFD model.*

CHAPTER IV  
RESULTS AND DISCUSSION

### Prototype Data

The data obtained from the prototype energy dissipating structure is presented in Table 1. Table 1 contains the values obtained from the anemometer in feet per minute in the first two columns and the values corrected for atmospheric pressure and converted to feet per second in the last two columns.

**Table 1** *Air Inlet Velocity Data Collected from Prototype.*

<b>Data Collected From Prototype</b>				
<b>Measurement #</b>	1	2	1	2
<b>Units</b>	FPM	FPM	FPS	FPS
<b>Atmosphere Correction</b>	No	No	Yes	Yes
<b>Position 1</b>	3051	3406	59.56	66.49
<b>Position 2</b>	2992	3602	58.41	70.31
<b>Position 3</b>	3071	3406	59.95	66.49
<b>Position 4</b>	2913	3622	56.86	70.71
<b>Position 5</b>	2870	3189	56.03	62.25
<b>Position 6</b>	3091	3209	60.34	62.64
<b>Position 7</b>	3051	3386	59.56	66.10
<b>Position 8</b>	3071	3642	59.95	71.10
<b>Position 9</b>	3130	3366	61.10	65.71
<b>Position 10</b>	2855	3287	55.73	64.17
<b>Position 11</b>	2972	3169	58.02	61.86
<b>Position 12</b>	3051	3406	59.56	66.49

Using the atmospheric corrected data in Table 1 and the process mentioned in the data process and handling section, volumetric air flow was calculated for the two different measurements. For the first column of measurements, the volumetric air flow came out to be 1414.92 cubic feet per second. For the second column of measurements, the volumetric air flow came out to be 1580.69 cubic feet per second. Figure 6 shows the

heatmap generated for the first column of data and Figure 10 shows the heat map generated for the second column.

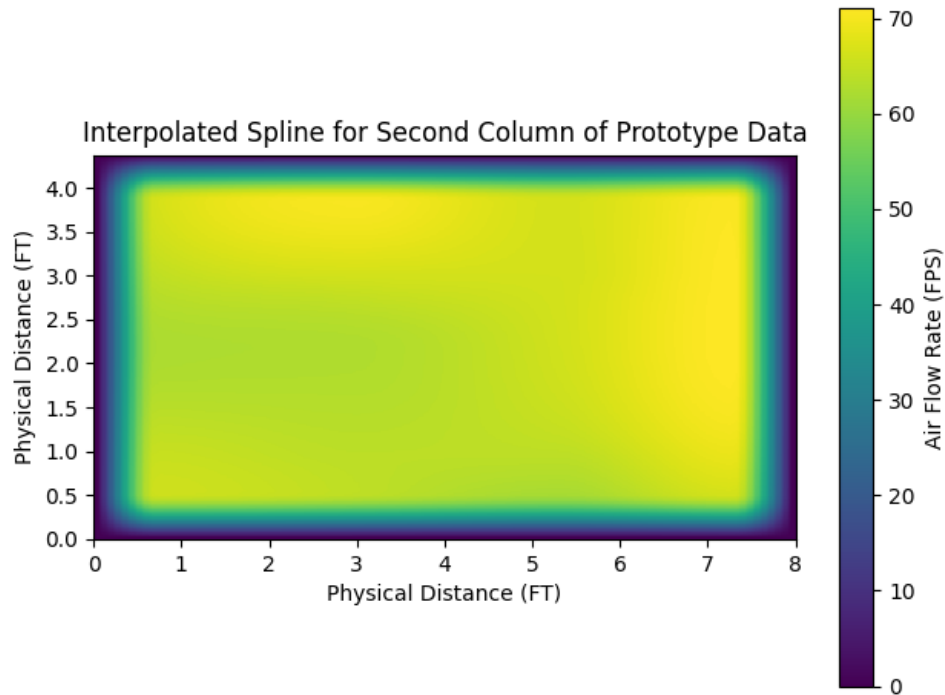


**Figure 10** *Spline-interpolated velocity for a prototype measurement (Column 4 in Table 1).*

### Model Data

The data obtained from the model built at Utah Water Research Laboratory is presented in Table 2. Table 2 contains the values obtained directly from the anemometer in feet per minute in the first two columns and the values corrected for atmospheric pressure and converted to feet per second in the last two columns.

**Table 2** *Air Inlet Velocity Data Collected from Scale Model.*

<b>Data Collected From Scale Model</b>				
<b>Measurement #</b>	1	2	1	2
<b>Units</b>	FPM	FPM	FPS	FPS
<b>Atmosphere Correction</b>	No	No	Yes	Yes
<b>Position 1</b>	112	53	2.19	1.04
<b>Position 2</b>	104	39	2.03	0.76
<b>Position 3</b>	106	35	2.07	0.68
<b>Position 4</b>	496	114	9.69	2.23
<b>Position 5</b>	569	382	11.11	7.46
<b>Position 6</b>	644	360	12.58	7.03
<b>Position 7</b>	624	325	12.19	6.35
<b>Position 8</b>	587	327	11.46	6.39
<b>Position 9</b>	705	404	13.77	7.89
<b>Position 10</b>	510	368	9.96	7.19
<b>Position 11</b>	646	437	12.62	8.53
<b>Position 12</b>	502	364	9.80	7.11

Using the data in Table 2 and the process mentioned in the data process and handling section, volumetric air flow was calculated for the two different measurements. For the first column of measurements, the volumetric air flow came out to be 2.36 cubic feet per second. For the second column of measurements, the volumetric air flow came out to be 1.34 cubic feet per second. Heatmaps for the interpolated spline data can be seen in Figures 11 and 12. As mentioned previously, an air velocity measurement using a 12-inch diameter tube placed over the grate was obtained for verification. That measurement gave an air flow rate of 2.8 cubic feet per second. Higher than the values given by the Jupyter Notebook, which is to be expected. However, it does show us that the measurements obtained weren't erroneously high due to drafts or water splashing onto the hot-wire anemometer. The second set of measurements is included for completeness, however being 43% lower than the first set of measurements is suspect.

This could've been caused by a curtain of water forming over the gate, smothering the air flow as mentioned in Elder and Daughtery (1953).

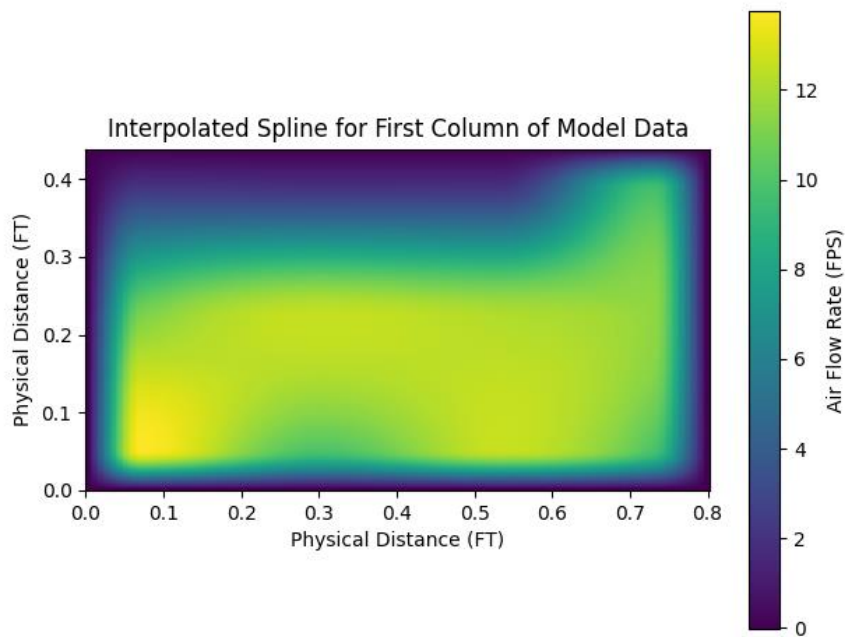


Figure 11 Spline-interpolated velocity for a model measurement (Column 3 in Table 2).

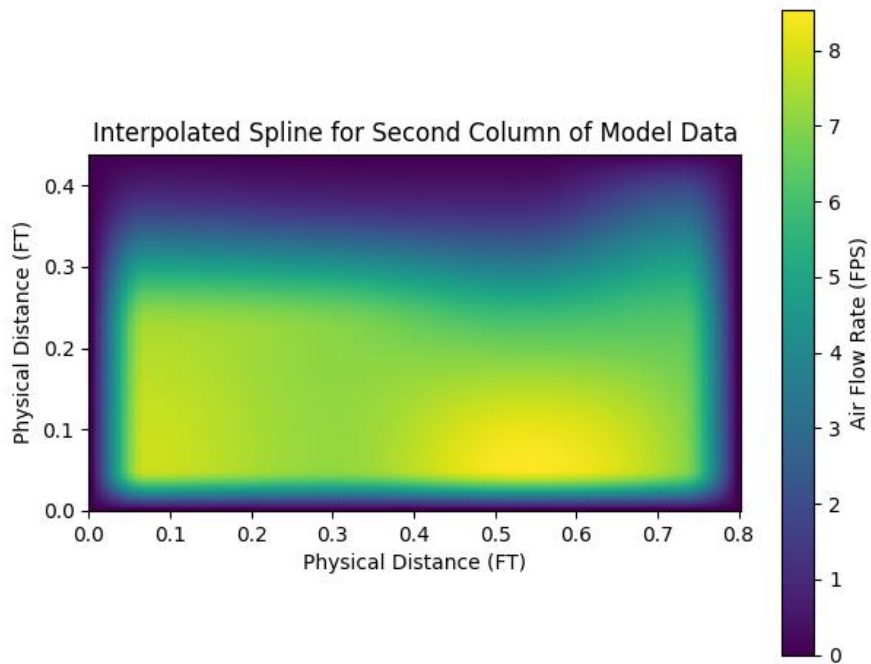


Figure 12 Spline-interpolated velocity for a model measurement (Column 4 in Table 2).

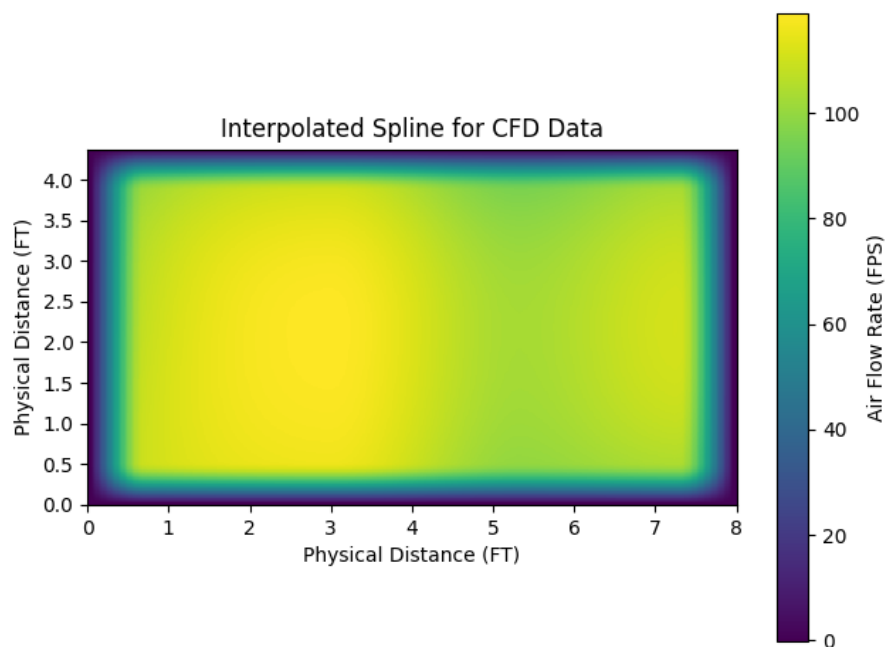
### **CFD Data**

The data obtained from the twelve monitoring points in the CFD simulation is presented above in Table 3. The measurements are given in feet per second. Using the data in Table 3, the volumetric air flow was calculated using the Jupyter Notebook. The value calculated was 2609.16 cubic feet per second. The heat map can be seen in Figure 13. The volumetric air flow across the stagnation inlet was also calculated using the values of a mass flow rate of 223.98 pounds per second and an air density of 0.0739 pounds per cubic foot. This gives a calculated rate of 3029.85 cubic feet per second, which is 420.69 cfs higher than the value calculated from the Jupyter Notebook. This is consistent with what we would expect using the interpolating spline and the boundary conditions of zero air flow on the edges of the grate. For comparison, the velocity seen in the CFD model across the air grate was obtained and can be seen in Figure 14. The CFD model has no velocity at the bars which is to be expected, however it has areas of negative flow. It should also be noted that the area of highest flow velocity is at the ends, which directly contradicts the assumption of the zero-flow boundary condition used in the interpolating spline.



**Table 3** Data Obtained from CFD Model (feet per second).

Data Collected From CFD	
Measurement #	1
Units	FPS
Position 1	102.04
Position 2	111.04
Position 3	95.55
Position 4	103.74
Position 5	108.25
Position 6	118.88
Position 7	103.14
Position 8	111.03
Position 9	109.81
Position 10	116.14
Position 11	99.94
Position 12	104.53

**Figure 13** Spline-interpolated velocity for CFD measurement (Table 3).

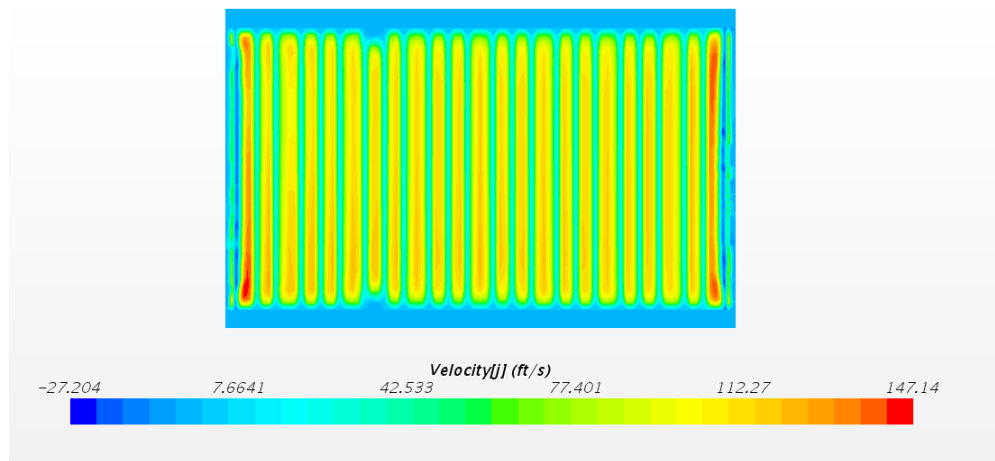


**Figure 14** Air velocity measurement using built in CFD tool.

### Prototype and Model Analysis

**Table 4** Calculated Air Flow Rates (Cubic Feet per Second).

Calculated Air Flow Rate	
	Air Flow (CFS)
<b>Prototype 1</b>	1414.92
<b>Prototype 2</b>	1580.69
<b>Model 1</b>	2.36
<b>Model 2</b>	1.34
<b>CFD</b>	2609.16
<b>CFD Mass Flow</b>	3029.85

Based off the laws of Froude similitude, it would be expected that the model air flow would scale to the prototype by 313 times. Using the larger value calculated for the air demand in the model of 2.36 cfs, this would only come out to a value of 738.68 cfs, much lower than the calculated average measured value of 1497.81 cfs. Using the corresponding high and low values of air demand from both the model and the prototype, a multiplicative factor between 669.78 and 1055.91 times is seen. Using the average values of 1.85 cfs and 1497.81 cfs gives a multiplicative factor of 809.62. For this particular energy dissipating structure, a scale effect between 2.14 and 3.37 times the quantity measured in the model is seen.

More importantly, comparing just the point velocities is critical as those are the values collected without any interpolation to get a volumetric flow rate. Froude similitude expects that the model air velocities would scale to the prototype air velocities by 3.16 times. Table 5 contains both the first column of measurements from the scale model as well as those measurements multiplied by the 3.16 Froude scaler. It can be seen that when compared to the average measurements taken from the prototype, each averaged prototype point velocity is between 1.5 and 10 times higher than the Froude scaled value, with the majority of them being between 1.5 and 2 times higher. The average of the scale effect comes out to be 3.71 times, which is slightly higher than the scale effect using the volumetric flow rates. The first three data points seem to be outliers and show the limitations of physical models. Not including those three outliers in the average for the scale effect gives a value of 1.74 times.

**Table 5** *Physical Model Data and Scaled via Froude Similitude. Includes Calculated Scale Effect.*

<b>Physical Model Data Scaled with Froude</b>				
<b>Measurement</b>	<b>1</b>	<b>1</b>	<b>Prototype Average</b>	<b>Calculated Scale Effect</b>
<b>Units</b>	FPS	FPS	FPS	
<b>Froude Scaled</b>	No	Yes	No	
<b>Position 1</b>	2.19	6.91	63.02	9.12
<b>Position 2</b>	2.03	6.42	64.36	10.03
<b>Position 3</b>	2.07	6.54	63.22	9.66
<b>Position 4</b>	9.69	30.61	63.78	2.08
<b>Position 5</b>	11.11	35.11	59.14	1.68
<b>Position 6</b>	12.58	39.74	61.49	1.55
<b>Position 7</b>	12.19	38.51	62.83	1.63
<b>Position 8</b>	11.46	36.22	65.52	1.81
<b>Position 9</b>	13.77	43.51	63.40	1.46
<b>Position 10</b>	9.96	31.47	59.95	1.90
<b>Position 11</b>	12.62	39.87	59.94	1.50
<b>Position 12</b>	9.80	30.98	63.02	2.03

It should also be noted that in a visual comparison of the heat map of the data collected from the model to the data collected from the prototype, it can easily be seen that the model heat map differs from the prototype. This difference could indicate the uncertainty in using model study to determine air flow rate in the prototype. Air compressibility and the limitations of capturing that using a Froude model may be a potential cause.

### **Prototype and CFD Analysis**

The CFD model produced a volumetric air flow rate of 2609.16 cfs, which is quite large in contrast to the volumetric air flow rates seen in the prototype of 1414.92 and 1580.69 cfs. Using the average of the prototype values, 1497.81 cfs, the CFD model produced an air demand 1.74 times that seen in the prototype.

Looking at just the comparison of air velocity measurements in the prototype and the CFD model produces Table 6. We can see in the column that is dividing the CFD air velocity by the averaged prototype air velocities for each point, the CFD velocities are around 1.5 to 1.94 times larger than the prototype. The average comes out to be that the CFD velocities are about 1.71 times larger than the values observed from the prototype. This is consistent with the air volume flow rates, which is expected as the air volume flow rate is calculated using the velocities as a base.

**Table 6** *CFD and Prototype Air Velocity Comparisons.*

CFD and Prototype Air Velocity Comparison					
Measurement #	1	1	2		
Units	FPS	FPS	FPS	FPS	
	CFD	Prototype	Prototype	Prototype Average	CFD/(Prototype Average)
<b>Position 1</b>	102.04	59.56	66.49	63.02	1.62
<b>Position 2</b>	111.04	58.41	70.31	64.36	1.73
<b>Position 3</b>	95.55	59.95	66.49	63.22	1.51
<b>Position 4</b>	103.74	56.86	70.71	63.78	1.63
<b>Position 5</b>	108.25	56.03	62.25	59.14	1.83
<b>Position 6</b>	118.88	60.34	62.64	61.49	1.93
<b>Position 7</b>	103.14	59.56	66.10	62.83	1.64
<b>Position 8</b>	111.03	59.95	71.10	65.52	1.69
<b>Position 9</b>	109.81	61.10	65.71	63.40	1.73
<b>Position 10</b>	116.14	55.73	64.17	59.95	1.94
<b>Position 11</b>	99.94	58.02	61.86	59.94	1.67
<b>Position 12</b>	104.53	59.56	66.49	63.02	1.66

The higher velocities in the CFD model is most likely due to inadequate computational power available to the researcher. Due to the large size of the computational domain, the model has 24,521,130 cells, which was roughly the maximum size that could be reached without Star-CCM+ crashing on the computer in use. Due to the limitation in cell count, a mesh refinement around the air vent was limited, which could've contributed to errors in the simulation. It should also be noted, the author noticed when performing mesh refinement around the gate of the fixed cone valve, the pressure in the fixed cone valve would rise as the cell count increased. A similar phenomenon occurred when decreasing the time step. Originally the time step was set at  $8e^{-5}$  seconds, however after correcting it to  $5e^{-5}$  seconds based off the Courant number calculation, the pressure at the fixed cone valve increased by around 5 psi. The potential for more accurate results may be achieved with a higher density mesh and a smaller time step. However, due to the long computational time required of smaller time steps and physical limitations of computer hardware, this was not feasible for this study.

It should also be noted that the heat maps produced from the prototype data and the CFD data follow a similar visual pattern. This is in contrast to the heat maps produced by the model data, which don't have the same consistency in air velocity across the entire grate. The model heatmaps produce a lower velocity near the top of the grate, while the prototype and CFD heat maps are more uniform. This implies that the CFD is doing a good job at modeling how the air flows throughout the structure but isn't necessarily capturing the correct volume of air flow. Future increases in access to higher computational power may allow CFD simulation to be a viable alternative to modeling air demand in fixed cone valves.

## CHAPTER V

### CONCLUSIONS

Fixed cone valves are widely used in reservoirs for low-level outlet discharge devices. To ensure optimal performance and to help prevent cavitation damage, air vents are required to supply air to the fixed cone valves. There is currently a lack of publicly available data in comparing model to prototype data to verify the usage of models in estimating prototype air demand for energy dissipating structures housing fixed cone valves. There is an additional lack of investigating the usage of using CFD software to accurately estimate air demand in hydraulic structures with fixed cone valves.

In this research, data was collected from both physical and numerical models to compare to data obtained from the field. The physical model was a 10 Froude model of the prototype energy dissipating structure. The CFD model was based off the full-size measurements of the prototype. Comparison of the data collected from the physical model and prototype was conducted. It was found that the data from the model would greatly underestimate the air velocities in the prototype by anywhere from 1.5 to 10 times too low. Due to this being the first publicly available prototype-model comparison, further collection of data from other sites with fixed cone valve installations is required to verify this result. Additionally, further research can look into the pressure gradient produced by the operation of the fixed cone valves and verifying the methodology used by Falvey (1980).

Data from the CFD model was also collected and compared to the values obtained from the prototype. It was found that the CFD model overestimated the air velocities compared to the prototype by around 1.71 times. A likely cause for this was due to the

limitations of computational resources available and time available to perform the research. Future research can be conducted with using different multiphase approaches such as using a Lagrangian Multiphase or different turbulence models. Future research could also be done using the same CFD models as used in this research, but with a finer mesh and smaller time steps.

A summary of key findings are as follows:

1. Data collected implies that Froude scaling does not apply to air flow in hydraulic structures. However, further data collected from more structures and at different flows is required.
2. Heat map comparison between model and prototype imply the model does not correctly capture the air flow throughout the structure.
3. Heat map comparison between CFD and prototype implies that the CFD simulation correctly captures the way air is flowing throughout the structure.
4. Number comparisons between CFD and prototype implies that CFD may not be a completely accurate tool to estimate the air demand in hydraulic structures, although it may be a reasonable, and in some cases the only available, tool engineers have to estimate air demand. However, further testing with more numerical model types and more computational resources is required.



## REFERENCES

- Calderon, D., Benavides, A. G., & Toro, F. M. (2018). CFD Simulation Of The Air-Water Flow In The Bottom Outlet Of Ituango Hydroelectric Project. *7th IAHR International Symposium on Hydraulic Structures*. Aachen, Germany.
- Colgate, D. (1963). *Hydraulic Model Studies of the River Outlet Works at Oroville Dam*. Denver, Colorado: Bureau of Reclamation.
- Elder, R. A., & Dougherty, G. B. (1953). Characteristics of Fixed-Dispersion Cone Valves. *Transactions of the American Society of Civil Engineers*, 907-927.
- Falvey, H. T. (1980). *Air-Water Flow in Hydrualic Structures*. Denver, Colorado: United States Department of the Interior.
- Harames, M. (2024). *Master Thesis Repository*. Retrieved from Github:  
<https://github.com/Harames/MastersThesis>
- Kanomax. (n.d.). *Anemomaster Model A031/A041/A034/A044 Operation Manual*. Retrieved April 2024, from [https://kanomax-usa.com/wp-content/uploads/2021/03/A031\\_Manual.pdf?x47665](https://kanomax-usa.com/wp-content/uploads/2021/03/A031_Manual.pdf?x47665)
- Scott, T. (2010, February 22). *Oroville Mercury-Register*. Retrieved from Report faults DWR in '09 dam accident: <https://www.orovillemr.com/2010/02/22/report-faults-dwr-in-09-dam-accident/>
- Siemens Digital Industries Software. (2018). *STAR CCM+ Documentation Version 13.04*. Plano, TX.